Received: 8 September 2023 | Revised: 15 December 2023 | Accepted: 27 December 2023

DOI: 10.1096/fj.202301836R

The FASEB Journal

RESEARCH ARTICLE

Induced pluripotent stem cell-derived extracellular vesicles enriched with miR-126 induce proangiogenic properties and promote repair of ischemic tissue

Katarzyna Kmiotek-Wasylewska[1] | **Anna Łabędź-Masłowska**[1] | **Sylwia Bobis-Wozowicz**[1] | **Elżbieta Karnas**[1] | **Sylwia Noga**[1,2] | **Małgorzata Sekuła-Stryjewska**[2] | **Olga Woźnicka**[3] | **Zbigniew Madeja**[1] | **Buddhadeb Dawn**[4] | **Ewa K. Zuba-Surma**[1]

[1]Faculty of Biochemistry, Biophysics and Biotechnology, Department of Cell Biology, Jagiellonian University, Kraków, Poland

[2]Malopolska Centre of Biotechnology, Laboratory of Stem Cell Biotechnology, Jagiellonian University, Kraków, Poland

[3]Faculty of Biology, Institute of Zoology and Biomedical Research, Department of Cell Biology and Imaging, Jagiellonian University, Kraków, Poland

[4]Department of Internal Medicine, Kirk Kerkorian School of Medicine, University of Nevada, Las Vegas, Las Vegas, Nevada, USA

Correspondence
Ewa K. Zuba-Surma, Faculty of Biochemistry, Biophysics and Biotechnology, Department of Cell Biology, Jagiellonian University, Kraków 30-387, Poland.
Email: ewa.zuba-surma@uj.edu.pl

Funding information
National Science Center of Poland (Narodowe Centrum Nauki), Grant/

Abstract

Emerging evidence suggests that stem cell-derived extracellular vesicles (EVs) may induce pro-regenerative effects in ischemic tissues by delivering bioactive molecules, including microRNAs. Recent studies have also shown pro-regenerative benefits of EVs derived from induced pluripotent stem (iPS) cells. However, the underlying mechanisms of EV benefits and the role of their transferred regulatory molecules remain incompletely understood. Accordingly, we investigated the effects of human iPS-derived EVs (iPS-EVs) enriched in proangiogenic miR-126 (iPS-miR-126-EVs) on functional properties of human endothelial cells (ECs) in vitro. We also examined the outcomes following EV injection in a murine model of limb ischemia in vivo. EVs were isolated from conditioned media from cultures of unmodified and genetically modified human iPS cells overexpressing miR-126. The iPS-miR-126-EVs were enriched in miR-126 when compared with control iPS-EVs and effectively transferred miR-126 along with other miRNAs to recipient ECs improving their functional properties essential for ischemic tissue repair, including proliferation, metabolic activity, cell survival, migration, and angiogenic potential. Injection of iPS-miR-126-EVs in vivo in a murine model of acute limb ischemia promoted angiogenesis, increased perfusion, and enhanced functional recovery. These observations corresponded

Abbreviations: AMI, acute myocardialinfarction; CLI, critical limb ischemia; copGFP, green fluorescent protein 2 from the copepod Pontellina plumata; ECs, endothelial cells; EVs, extracellular vesicles; hSF-EVs, human skin fibroblast–derived extracellular vesicles; hSFs, human skin fibroblasts; IHD, ischemic heart disease; iPS, induced pluripotent stem cells; iPS-copGFP, induced pluripotent stem cells expressing copGFP; iPS-copGFP-EVs, extracellular vesicles from induced pluripotent stem cells expressing copGFP; iPS-EVs, induced pluripotent stem cell–derived extracellular vesicles; iPS-miR-126, induced pluripotent stem cells enriched in miR-126; iPS-miR-126-EVs, extracellular vesicles from induced pluripotent stem cells enriched in miR-126; iPS-WT, unmodified (wild type) induced pluripotent stem cells; iPS-WT-EVs, extracellular vesicles from unmodified induced pluripotent stem cells; MSCs, mesenchymal stem cells; SCs, stem cells.

Award Number: 2019/34/A/NZ3/00134 and 2016/21/N/NZ3/00363

with elevated expression of genes for several proangiogenic factors in ischemic tissues following iPS-miR-126-EV transplantation. These results indicate that innate pro-regenerative properties of iPS-EVs may be further enhanced by altering their molecular composition via controlled genetic modifications. Such iPS-EVs overexpressing selected microRNAs, including miR-126, may represent a novel acellular tool for therapy of ischemic tissues in vivo.

KEYWORDS

angiogenesis, extracellular vesicles, induced pluripotent stem cells, ischemic injury, miR-126, regeneration

1 | INTRODUCTION

Ischemic pathologies, including ischemic heart disease (IHD) and critical limb ischemia (CLI), represent leading causes of death and morbidity in developed societies, indicating their prevention and treatment as one of the main challenges of modern medicine.[1] Despite the current pharmacotherapy and surgical interventions, novel therapeutic strategies are badly needed to prevent diverse adverse effects of ischemic tissue damage and to restore functionality of injured organs.

Growing evidence supports that stem cell (SC)-based therapies represent promising approaches for the treatment of ischemic diseases.[2,3] Importantly, it has been reported that SC-mediated pro-regenerative effects in injured tissues are largely due to the release of regulatory paracrine factors such as cytokines, growth factors, and extracellular vesicles (EVs).[4,5] Recent data suggest an important role of especially the SC-derived EVs in tissue repair by concurrent transfer of several bioactive molecules into cells residing in injured tissues. It has been reported that these natural inter-cellular nanocarriers may carry active proteins, lipids, and nucleic acids including regulatory microRNAs, which modulate functions of recipient cells.[6,7] We have recently shown that not only adult SCs such as mesenchymal stem cells (MSCs) or cardiac progenitor cells, but also induced pluripotent stem (iPS) cells may release EVs promoting ischemic tissue repair, including heart regeneration.[8–10] In our previous studies, we demonstrated that iPS-derived EVs (iPS-EVs) lead to improvement of anatomy and function of infarcted heart after their in vivo administration following acute myocardial infarction (AMI) in mice.[8] We indicated an important role of several iPS-EV-derived miRNA molecules in regulating the pro-regenerative processes in heart tissue including angiogenesis and cell survival in cytotoxic environment.[8,10]

Small non-coding RNAs such miRNAs have been postulated to mediate a functional impact on recipient cells among various bioactive compounds present in the EV cargo. MicroRNAs maintain cell homeostasis in normal tissues, but may also regulate various processes related to tissue repair and regeneration, including cell proliferation, differentiation, apoptosis, and survival.[11–13] One of pivotal miRNA regulating angiogenesis is miR-126, shown to play an important role in neovascularization and blood vessel stabilization.[14,15] It has been shown that miR-126 overexpression in cells leads to increased proliferation, migration, and capillary formation capacity of endothelial cells (ECs) both in vitro and in vivo.[16,17] Considering this, the aim of this study was to examine whether fortification of iPS-EVs with miR-126 may enhance EC function in vitro and salvage ischemic limb following transplantation in vivo has not been investigated before.

2 | MATERIALS AND METHODS

2.1 | Cell culture

Human iPS cell lines, including (i) unmodified iPS cells generated in our laboratory (iPS-WT),[10] (ii) genetically modified cells overexpressing miR-126 (iPS-miR-126), and (iii) control copGFP overexpressing cells (iPS-copGFP), were cultured in feeder-, serum-, and xeno-free conditions in Essential 8 Medium (Gibco/Thermo Fisher Scientific, Waltham, MA, USA) supplemented with penicillin (100 U/mL) and streptomycin (100 μg/mL) solution (P/S, Gibco) on culture plates coated with rhVitronectin (50 μg/mL; Gibco). The media was changed every day. Every four days cells were passaged using 0.5 mM EDTA (Invitrogen/Thermo Fisher Scientific) and seeded in medium containing 10 μM/mL Rho-associated protein kinase inhibitor (Y-27632, Sigma-Aldrich/Merck, St. Louis, MO, USA) for 24 h.

Human primary endothelial cells (ECs) represented by human coronary artery ECs (HCAECs) derived from 57-year-old female donor were purchased from Lonza (Lonza, Basel, Switzerland) and were cultured in our

laboratory in dedicated Microvascular Endothelial Cell Growth Medium-2 (EGM-2MV, Lonza). The cells used in experiments were on early stage of culture (passage 4).

Control human cells represented by primary normal human dermal fibroblasts from adult donor (NHDF-Ad), derived from 22-year-old male donor, were purchased from Lonza and were cultured in dedicated Fibroblast Growth Medium-2 (FGM-2, Lonza). Since the cells were used for EV harvest, the medium was first ultracentrifuged for 18 h, in 4°C at 100 000×*g* to remove any endogenous EVs present in the media components ("EV depleted medium"). The cells used in experiments were on early stage of culture (only early passages 3–5 were used for EV harvest).

2.2 | Lentivirus production and generation of stable cell lines expressing miR-126

Lentiviral expression vector for human pre-miR-126 (pHMIR126) was purchased from Systems Biosciences (Palo Alto, CA, USA). Additionally, control vector (pHMIR-copGFP) expressing copepod green fluorescent protein (copGFP) was created by deletion of CMV7 promoter with miRNA sequence from pHMIR126 plasmid by Spe I and Not I digestion (both from New England Biolabs, Ipswich, MA, USA). DNA ends were then linked with the Quick blunting Kit (New England Biolabs) and ligated with the T4 DNA Ligase (Thermo Fisher Scientific).

Lentiviral vectors were produced in HEK293T/17 packaging cell line (ATCC-CRL-11260; LGC Standards, Teddington, UK). Cells were co-transfected using Lipofectamine 2000 transfection reagent (Invitrogen) with pHMIR-126/pHMIR-copGFP together with packaging plasmids—psPAX2 and pMD2G (#12260 and #12259, respectively; Addgene, Cambridge, MA, USA). Supernatants collected from cell cultures were then filtered through 0.2-μm pore PVDF filters (Millipore/Merck) and used for infecting iPS cells (MOI = 5) in Essential 8 Medium and with addition of 10 μg/1 mL of polybrene (Millipore). Cells were then expanded for at least 6 days, and then, copGFP-expressing cells were sorted with FACS Aria III cell sorter (BD Biosciences, San Jose, CA, USA).

2.3 | Isolation of extracellular vesicles

Conditioned media from iPS-WT, iPS-copGFP, and iPS-miR-126 and control NHDF-Ad cells were collected for EV isolation at 80%–90% of cell confluency. EVs were isolated according to sequential centrifugation protocol, as we have previously described.[10] Briefly, conditioned media were centrifuged at 2000×*g* for 20 min (4°C) to remove cellular debris. Collected supernatants were then ultracentrifuged at 100 000×*g* for 70 min (4°C) using 50.2Ti rotor and Optima XPN-90 ultracentrifuge (both from Beckman Coulter, Brea, CA, USA). EV pellets were washed with PBS (Lonza) and spun again in same conditions. The obtained EV pellets were re-suspended in 100 μL of PBS. Protein concentration was determined in EV samples with the Bradford assay.

2.4 | Nanoparticle tracking analysis (NTA)

Particle size distribution and concentration of EVs in samples were measured with the NanoSight NS 300 nanoparticle analyzer (NanoSight, Malvern, Worcestershire, UK) based on Brownian movement of particles. EV samples were diluted in PBS (1:1000) before the measurement for optimal particle count (1×10^8 to 1×10^{10}). Using the script control function in NTA 2.0 Software (Malvern), three 60-s videos were recorded and analyzed for each sample. All data were collected with camera level set to 13 and detection threshold set to 3.

2.5 | Transmission electron microscopy (TEM)

EVs were stained using negative staining procedure for imaging. 20 μL of EV sample was added to TEM nickel grids (Agar Scientific, Stansted, UK) for 30 min. EVs attached to grids were then fixed for 5 min with 2.5% glutaraldehyde solution (Sigma). The grids were next washed with PBS, blotted with filter paper, and stained twice with 2% uranyl acetate (Agar Scientific) for 30 min. Next, grids were washed three times with distilled water and air-dried. EVs were visualized by JEOL JEM2100 HT CRYO LaB6 transmission electron microscope (JEOL, Peabody, MA, USA).

2.6 | Proliferation analysis

The EC proliferation after EV treatment was examined using the colorimetric Cell Counting Kit-8 (Sigma-Aldrich, Merck Darmstadt, Germany) according to the manufacturer's protocol. Accordingly to the product data sheet provided by manufacturer, correlation between CCK8 and (3H)-thymidine incorporation assay is high ($r = .999$ for HeLa cells, $r = .996$ for HL60 cells) indicating that CCK-8 is a suitable assay for evaluating cell proliferation and is broadly used in several studies.[18,19]

ECs were seeded in EGM-2MV medium and after 24 h were treated with EVs in concentration of 20 ng/1000 cells; 200 ng/mL of medium for 24 h, while corresponding volume of PBS was added to untreated samples, acting as a vehicle control. Cell proliferation was evaluated 24, 48, and 96 h after EV treatment in both standard (21% O_2) and hypoxic (1% O_2, dual-gas incubator) conditions. Absorbance was measured at 450 nm using Multiskan FC Microplate Photometer (Thermo Fisher Scientific).

2.7 | Metabolic activity analysis

The rate of ATP production in ECs was measured using ATPLite Kit (PerkinElmer Waltham, MA, USA) following the manufacturer's protocol. ECs were seeded in EGM-2MV medium and after 24 h were treated with EVs in concentration of 20 ng/1000 cells; 200 ng/ mL of medium for 24 h, while corresponding volume of PBS was added to untreated samples, acting as a vehicle control. Metabolic activity measured by ATP level was evaluated at 24, 48, and 96 h after EV treatment in cells cultured in both standard (21% O_2) and hypoxic conditions (1% O_2, dual-gas incubator). Luminescence was measured using the Infinite M200 Microplate Reader (Tecan, San Jose, CA, USA).

2.8 | Apoptosis analysis

To evaluate both EV anti-apoptotic and cytoprotective effects on ECs, two (2) following experimental variants were performed. First, to assess cytoprotective effect of EVs, ECs were seeded on 6-well plates and then treated with EVs (20 ng/1000 cells; 1000 ng/ 1 mL of medium) for 24 h. Next, apoptosis was induced by addition of 1 μM staurosporine (Santa Cruz Biotechnology, Dallas, TX, USA) for 6 h. Second, to assess anti-apoptotic impact of EVs, ECs were seeded for 24 h and next treated with 1 μM of staurosporine for 6 h, which was followed by treatment with EVs (20 ng/1000 cells) for 24 h. Apoptosis was measured using the CellEvent Caspase-3/7 Green Detection Reagent (Thermo Fisher) according to the manufacturer's protocol, on LSRFortessa flow cytometer and analyzed with BD FACSDiva ver. 8.1 Software (both from BD Biosciences, Franklin Lakes, NJ, USA).

2.9 | Migration analysis

To evaluate an impact of EVs on EC migratory potential, ECs were seeded on 12-well plates at density of 20 000 cells per well in EGM-2MV medium. After 24 h, cells were treated with EVs (20 ng/1000 cells; 400 ng/1 mL of medium) and placed under Leica DMI6000B microscope (Leica Biosystems, Wetzlar, Germany) equipped with DFC360FX CCD camera (Leica), where migratory activity was recorded for 12 h with 10-min intervals (at 37°C and 5% CO_2). Cell trajectories were constructed from a sequence of cell centroid positions, pooled, and analyzed with the Hiro program (written by W. Czapla). Two hundred different, independent cells per each condition were analyzed to assess the average speed of cell movement (μm/h) and total length of traveled distance and cell displacement (both in μm).

2.10 | Capillary formation assay in vitro

To measure proangiogenic properties of EVs on ECs, the cells were seeded on 24-well plates coated with Matrigel Matrix Growth Factor Reduced (BD Biosciences), more suitable for this assay, as it does not contain growth factors, that are known to over-stimulate ECs.[20] GFR Matrigel was used in concentration of 100 μL/well. Cells were next treated with EVs (20 ng/1000 cells; 400 ng/1 mL of medium) and analyzed using Leica DMI6000B microscope (Leica). Pictures of forming capillaries were taken for 9 h at 30-min intervals, at 37°C and 5% CO_2. For each condition, the number of fully closed and fully visible capillaries was "blindly" counted on 15 independent pictures per condition per time point. An average number of formed capillaries per field of view, considered a standard way of reporting results from capillary formation assay,[21,22] were calculated for each time point.

2.11 | High-resolution imaging flow cytometry

Samples of iPS-EVs were stained with RNASelect dye (Thermo Fisher Scientific) and APC-conjugated antibodies against human: tetraspanins CD9, CD63, and CD81, stage-specific embryonic antigen-4 (SSEA-4), and CD34 as a negative control for 30 min at 4°C (Table S1). Analysis was performed with an Apogee A60-Micro high-resolution flow cytometer (Apogee Flow Systems, Hemel Hempstead, UK), calibrated before every acquisition with using Apogee calibration beads (#1493; Apogee Flow Systems). The percentage of RNASelect-gated particles expressing indicated surface marker was calculated by Apogee Software (Apogee Flow Systems). Appropriate isotype controls were included in the gating strategy. Additionally, stained iPS-EVs were imaged using imaging flow cytometer ImageStreamX Mk II (Luminex Corp., Austin, TX, USA) under 60× objective magnification and analyzed in IDEAS Software (Luminex Corp., Austin, TX, USA).

2.12 | Quantitative real-time PCR analysis

Total cellular and vesicular RNA was isolated using miRCURY RNA Isolation Kit—Cell & Plant (Exiqon/Qiagen, Hilden, Germany). Samples were collected via direct lysis, on well/ EV prep sample, using ice-cold kit provided lysis buffer. After lysate collections, RNA was immediately isolated according to the manufacturer's protocol. Murine muscle tissue samples were collected and snap-freezed in LN stored at −80°C until isolation. Total RNA was isolated using TRIzol (Thermo Fisher Scientific) with additional tissue homogenization step, using hand homogenizer. cDNA synthesis was performed with NG dART RT Kit (EURx, Gdansk, Poland) for mRNA analysis and Universal cDNA synthesis Kit II (Exiqon) for miRNA analysis, according to the manufacturers' instructions. Transcript levels were evaluated using the real-time quantitative PCR method by the QuantStudio 6 Flex Real-Time PCR System (Thermo Fisher Scientific) using the ΔΔCt method with β-2-microglobulin as an endogenous control for mRNA and U6 snRNA as an endogenous control for miRNA analysis. Since identification of reliable endogenous control for EVs studies is difficult, due to selective content sorting, as reported by Gouin et al.[23], for expression comparison between EVs and parent cells, we analyzed ratio of normalized Ct cycle. For each reaction, SYBR Green Master Mix (Applied Biosystems/Thermo Fisher Scientific) and specific primer sets were used for cellular gene expression studies (Table S2), while RT^2 Profiler PCR Array Mouse Angiogenesis (Qiagen) panels were used to examine angiogenesis-related gene expression in animal tissues (Table S3). For miRNA expression analysis, Power SYBR Green Master Mix (Applied Biosystems/Thermo Fisher Scientific) with specific anti-miR LNA primers (Exiqon) was used.

2.13 | Murine model of acute limb ischemia in vivo

All animal procedures were conducted under the approval of II Local Ethical Committee (II LKE) in Krakow (approval number 323/2017) and were performed in accordance with all relevant guidelines and regulations. In our study, we used 8- to 10-week-old SCID mice (strain: CB17/Icr-Prkdc<scid>/IcrIcoCrl; Charles River Laboratory), which correspond to adult animals, and the age of mice (6- to 12-week-old) used by other investigators in their studies employing limb ischemia model in regeneration studies.[24–26] The mice underwent acute limb ischemia by femoral artery occlusion according to a protocol developed by Niiyama et al.[27] Briefly, after skin incision, femoral artery was permanently ligated and cut. The skin was closed using sutures. Total volume of 50 μL of PBS (control) or indicated EV sample (containing 1.0×10^{10} of EVs) was injected intramuscularly (5 injections of 10 μL) in ischemic region after 24 h post-surgery.

Macroscopic observations of animals' weight, mobility (Table S4), and limb anatomy and condition (Table S5) were performed by blinded investigator daily for 4 weeks. Blood perfusion in healthy and treated limbs was measured by Laser Doppler Perfusion Imager PeriScan PIM 3 (Perimed AB, Stockholm, Sweden) at 0, 1, 7, 14, 21, and 28d after treatment with EVs. Briefly, mice were anesthetized prior to measurements and their body temperature was maintained on 37°C by placing on heating pad. Collected data were analyzed using LDPI win Software (Perimed AB). Animals were sacrificed at 28d of follow-up, and limb muscle tissues were harvested and snap-freezed for further molecular analysis.

2.14 | Statistical analyses

At least three experiments were performed in duplicate for each study. The data are presented as means ± standard deviations (*SD*). Statistical analyses were done with unpaired Student's *t*-test or one-way ANOVA and Tukey's multiple comparison test using GraphPad Prism7 (GraphPad Software, La Jolla, CA, USA). p values of <.05 were considered statistically significant ($^*p<.05$; $^{**}p<.01$; and $^{***}p<.001$).

3 | RESULTS

3.1 | Genetically modified iPS cells express high levels of transgenic miRNA while maintaining pluripotent phenotype

Since the main aim of this study was to examine proangiogenic properties of EVs derived from genetically modified iPS cells overexpressing miR-126, we first generated and characterized transgenic iPS cell lines. Human native (wild type) iPS cells (iPS-WT) used in this study have been previously established and characterized in our laboratory by Bobis-Wozowicz et al.[10] The cells were next transduced using lentiviral vectors to overexpress proangiogenic miR-126 (iPS-miR-126) along with a selection fluorescent marker protein (copGFP), allowing cell selection and monitoring of transgene expression (Figure 1A). Control iPS cells expressing only copGFP (iPS-copGFP) were generated with a control vector (with no miRNA sequence). To evaluate transduction efficiency, we used

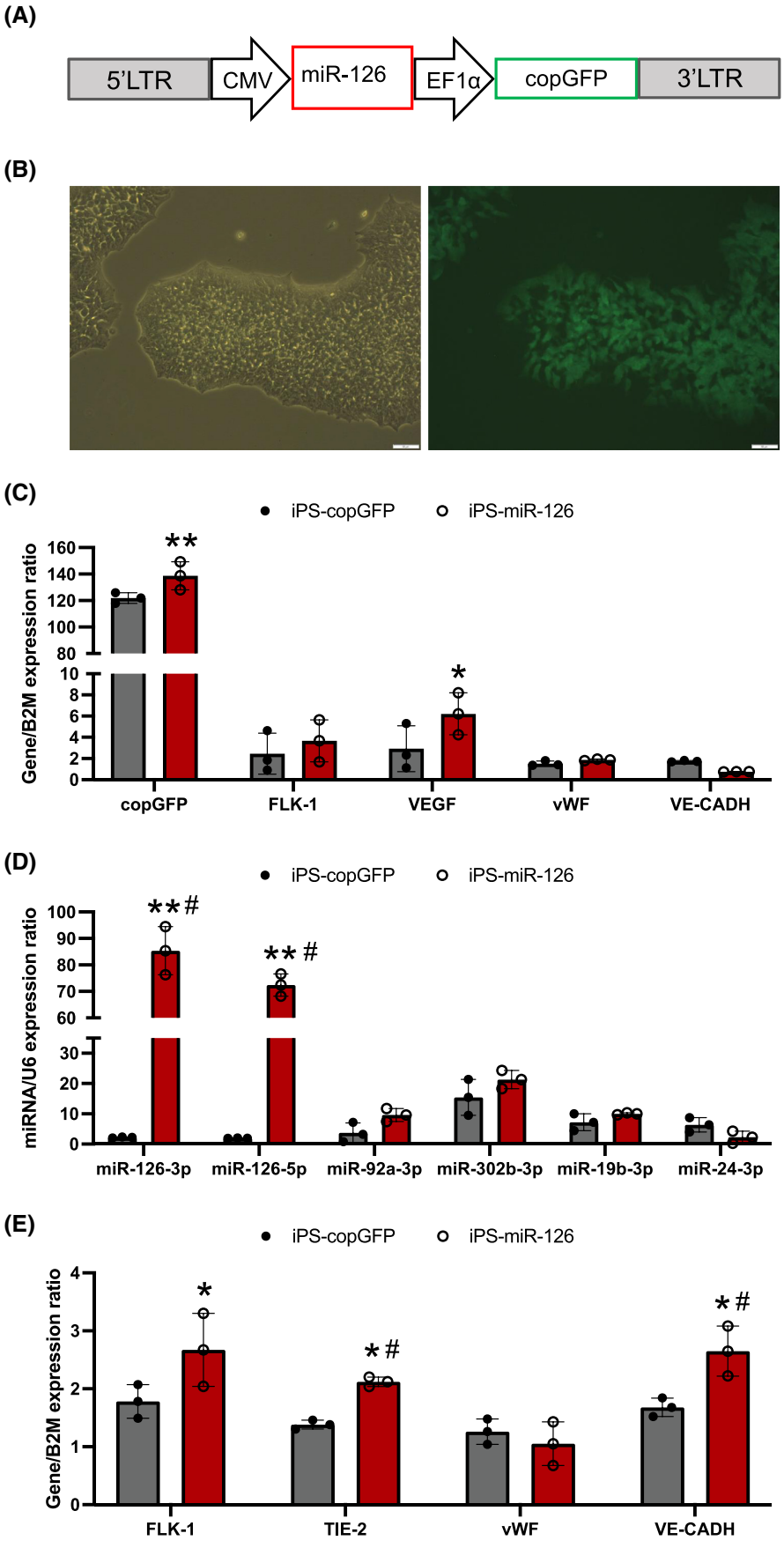

FIGURE 1 Generation of iPS cell transgenic line overexpressing miR-126. (A) Schematic representation of lentiviral vector carrying miR-126 used for transduction. LTR—long terminal repeat, CMV—cytomegalovirus promoter, EF1α—elongation factor 1 alpha gene promoter, and copGFP—variant of a green fluorescent protein derived from copepepod *Pontellina plumata*. (B) Representative microscopic images of iPS cells genetically modified to express miR-126 and co-expressing copGFP. (C) Analysis of relative mRNA expression levels of copGFP and early (FLK-1, VEGF) and late (vWF, VE-CADH) genes related to angiogenesis in genetically engineered iPS cell lines using RT-qPCR. (D) Analysis of relative miRNA expression levels of miR-126 and selected miRNAs related to cell pluripotency and proliferation in iPS-miR-126 cells when compared to control cell lines using RT-qPCR. (E) Analysis of mRNA levels for early (FLK-1, TIE-2, VEGF) and late (vWF, VE-CADH) angiogenesis-related genes in genetically engineered iPS cell lines after 7 days of angiogenic differentiation. Mean ± *SD*; $n = 3$; ANOVA with Tukey post-hoc test; comparison with iPS-WT control cell line; $^{*}p < .05$, $^{**}p < .01$; comparison with iPS-copGFP control cell line; $^{\#}p < .05$.

fluorescence microscopy and confirmed presence of transduced cells in treated populations by copGFP expression (Figure 1B). Moreover, high levels of copGFP and overexpressed miR-126-3p and miR-126-5p variants were also quantitatively confirmed in genetically modified iPS cells using real-time qPCR (Figure 1C,D). Importantly, we did not observe any change in the expression of other miRNAs including the selected ones regulating pluripotency and cell proliferation (Figure 1D), which indicates sustained pluripotency status of our genetically modified iPS cells.

Next, we evaluated an impact of miR-126 overexpression on activation of angiogenesis related genes in the genetically modified iPS cells, including transcription factor TIE-2, von Willebrand factor (vWF), VE-cadherin (VE-CADH), and vascular endothelial growth factor (VEGF) and its receptor FLK-1. We found that all iPS cell lines exhibit relatively high expression of early angiogenesis-related genes (FLK-1, TIE-2) and low level of late angiogenesis-related genes (vWF, VE-CADH) confirming their developmentally early status, which was not related to miR-126 overexpression. However, iPS-miR-126 cells exhibited significantly higher expression of VEGF when compared to controls (Figure 1C). VEGF is one of the main growth factors involved in angiogenesis,[28,29] and its high expression in parental iPS cells may potentially enhance properties of their EVs. Importantly, we also found significantly increased expression of proangiogenic genes in iPS-miR-126 cells when differentiating in angiogenesis-promoting medium, as compared to controls (Figure 1E), which suggest increased angiogenic potential of iPS cells overexpressing miR-126.

3.2 | Genetically modified iPS-EVs carry proangiogenic mRNAs and miRNAs

To verify whether overexpressed miR-126 may be transferred from parental iPS cells to vesicles, iPS-EVs were first isolated from conditioned media using the sequential centrifugation method with an ultracentrifugation step and further characterized according to International Society of Extracellular Vesicles (ISEV) guidelines.[30] Particle size distribution analysis with NTA revealed average size of vesicles to be between 130 and 210 nm, with iPS-EVs harvested from genetically modified iPS cell lines being more heterogeneous and larger when compared to iPS-WT-EVs (Figure 2A, Table S6). It has been proven that genetic manipulation, staining, and electroporation may impact EV size, which would be consistent with our findings.[31] Additionally, particle-to-protein ratio was analyzed within EV samples to confirm similar purity of the EV isolates (Table S7). The presence of small (around 100–120 nm in diameter), round membrane vesicles in our EV isolates was also confirmed by TEM (Figure 2B).

The presence of typical EV markers was confirmed on iPS-EVs by phenotypic analysis with high-resolution flow cytometry. iPS-EVs were also stained prior to analysis using RNASelect dye, which binds to RNA molecules, and only integral vesicular objects were further gated and analyzed (Figure 2D). We found that EVs isolated from both control and miR-126-overexpressing iPS cells contain similar percent content of vesicles expressing typical exosomal markers such as tetraspanins CD81, CD63, and CD9,[32] with CD81 being the most abundant (Figure 2E). They also contain similar percentage of vesicles expressing surface markers of parental iPS cells such as, for example, SSEA-4, suggesting similar ectosomal content within all iPS-EV specimens. All tested iPS-EVs were also negative for CD34 marker, which served as a negative control (Figure 2E). The expression of selected EV markers was also confirmed on iPS-EVs using imaging flow cytometry platform ImageStreamX Mk II (Figure 2C).

Finally, we analyzed the contents of overexpressed miR-126 and selected angiogenesis-related mRNA transcripts in EVs from genetically modified iPS cells in order to compare them with parent cells. We found similar levels of miR-126 and selected mRNAs in iPS-EVs and their parental iPS cells (Figure 2F,G). Stability of B2M and U6 as housekeeping genes across various analyzed EV samples for mRNA and miRNA analyses, respectively, is shown in Table S8.

Thus, we showed that EVs isolated from genetically modified iPS cells meet criteria of ISEV and that miR-126 can be effectively transferred from iPS cells to the cargo of iPS-miR-126-EVs.

3.3 | iPS-miR-126-EVs enhance metabolic activity, migration, survival, and angiogenic potential of endothelial cells in vitro

To evaluate a functional impact of genetically modified iPS-miR-126-EVs on endothelial cells, we first examined proliferation of ECs treated with iPS-EVs in both normoxic (21% O_2) and hypoxic conditions (1% O_2), mimicking environment of an ischemic injured tissue. We observed decreased proliferation of ECs at 24, 48, and 96 h after iPS-miR-126-EV treatment when compared to controls. Reduced proliferation of ECs was observed in both standard normoxic and hypoxic conditions (Figures 3A, S3A, and Table S9).

Next, we analyzed impact of genetically modified iPS-EVs on metabolic activity of ECs by measuring ATP production in these cells in both normoxic (21% O_2) and

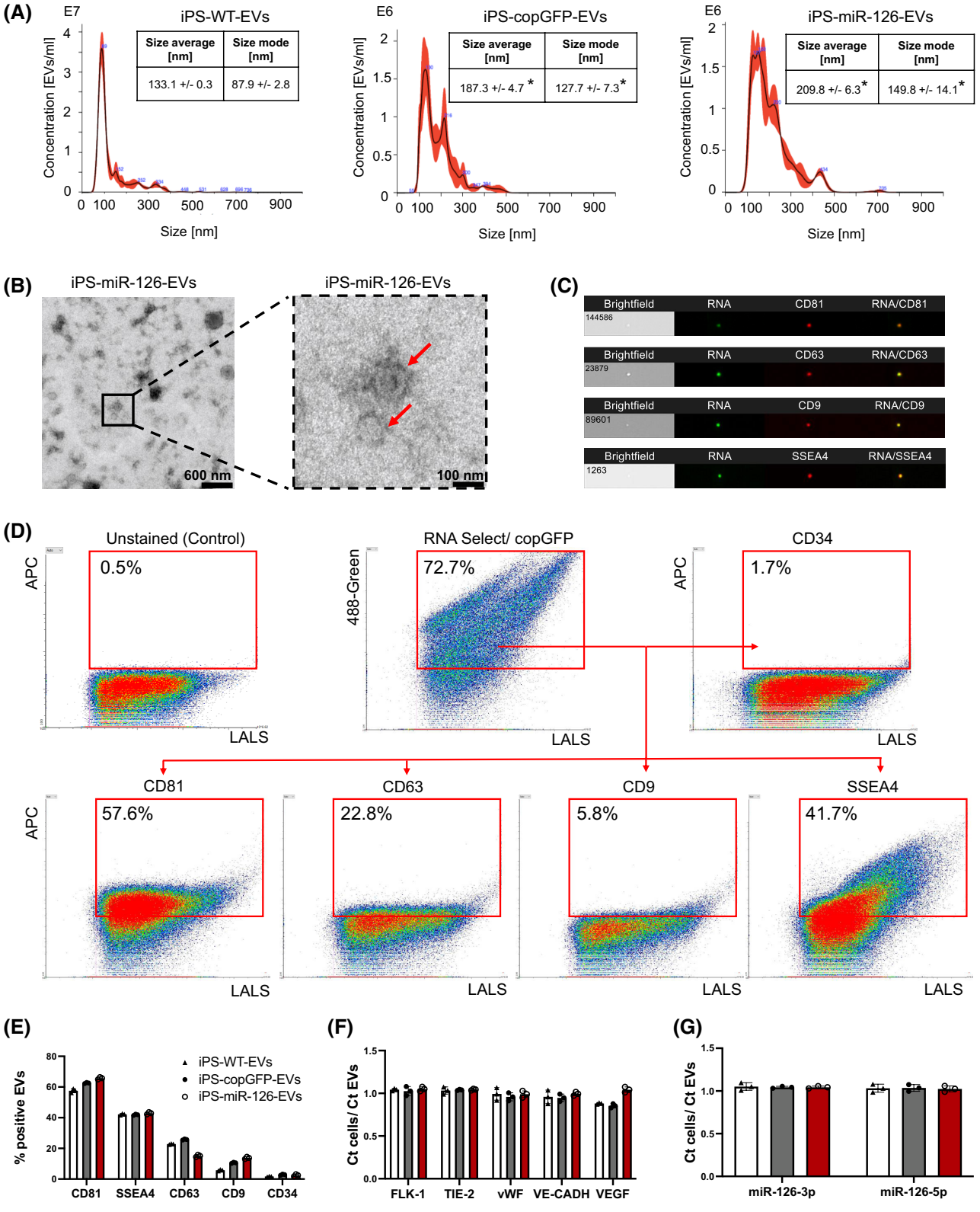

hypoxic conditions (1% O_2). No change in metabolic activity was observed in normoxic conditions following the treatment with all iPS-EVs. However, significant increase of ATP production was observed in ECs treated with iPS-miR-126-EVs in hypoxic conditions at 24 and 96 h after treatment (Figures 3B, S3B, and Table S10).

Since effective migratory capacity of ECs may be critical for their functional properties required in tissue healing and repair, as well as for their ability for new vessel formation and maturation,[33] the potential impact of iPS-miR-126-EVs on migration of ECs was examined when compared to control EVs. EC migration was monitored for

FIGURE 2 Characterization of iPS-EVs stably expressing miR-126. (A) Particle size distribution in EV samples from control and genetically modified iPS cells by nanoparticle tracking analysis (NTA). Representative graphs, average, and mode size are presented. (B) Representative image of iPS-miR-126-EV sample along with the selected magnified section of the image by transmission electron microscopy (TEM). Red arrows indicate EVs. (C) Representative images of single iPS-EVs with RNA (green) and selected iPS-EV markers (red), captured in brightfield and fluorescence channels by imaging cytometry. The objective with 60× magnification was used for the acquisition. The number in a left upper corner of BF image is an object number from ImageStreamX Mk II gallery. (D) Analysis of selected markers expression in iPS-EV population by high-resolution flow cytometry. Representative dot-plots of iPS-EV samples with RNA and stained with fluorescent antibodies, acquired by Apogee A60-Micro flow cytometer. The percentages of objects positive for the analyzed markers are shown in red gates. LALS—large angle light scatter parameter, corresponding to the relative size of analyzed particles. (E) Quantitative data for iPS-EV antigenic phenotyping with high-resolution flow cytometry. (F) Relative expression levels of early (FLK-1, TIE-2, VEGF) and late (vWF, VE-CADH) genes related to angiogenesis in iPS-EVs when compared to parental iPS cells by RT-qPCR. (G) Relative expression levels of miR-126 variants in iPS-EVs when compared to parental iPS cells by RT-qPCR. Mean ± *SD*; $n = 3$; ANOVA with Tukey post-hoc test; comparison with iPS-WT-control cell lines; $^{*}p < .05$, $^{**}p < .01$; comparison with iPS-copGFP control cell line; $^{\#}p < .05$.

12 h after EV treatment and was followed by quantitative analysis of recorded migration trajectories based on time-lapse monitoring of spontaneous and unguided movement of single cells (Figure 4A). We observed enhanced migratory activity of ECs upon stimulation with iPS-miR-126-EVs as showed by significantly increased cell migration speed, speed of displacement, and migration distance (Figure 4A).

Following cell migration analysis, we performed capillary-like tube formation assay in vitro that allowed examining EC angiogenic potential after iPS-EV treatment, as shown by representative image of capillaries formed on Matrigel (Figure 4B). The quantitative data have revealed a significant increase in the number of capillaries formed by ECs co-incubated with iPS-miR-126-EVs when compared with untreated cells or ECs treated with control iPS-WT-EVs or iPS-copGFP-EVs, as examined at different time points of the assay (Figure 4B).

To further investigate a potential impact of miR-126-EVs on viability and survival of ECs in cytotoxic conditions, we subjected these cells to two distinct protocols combining treatment with cytotoxic agent (staurosporine) and iPS-EVs, to measure both antiapoptotic and cytoprotective effects of EVs. Firstly, to verify antiapoptotic properties of EVs, ECs were subjected to the treatment with staurosporine followed by incubation with iPS-EVs. Using classical flow cytometry, we found significantly increased percentage of viable cells among ECs treated with iPS-miR-126-EVs, when compared to control staurosporine-treated cells (Figure 4C, left). Such antiapoptotic effects in ECs were not observed for control iPS-WT-EVs or iPS-copGFP-EVs, suggesting that the presence of miR-126 in iPS-EV may enhance their inhibitory regulation of apoptosis induced in ECs. Secondly, to study possible cytoprotective effects of EVs on ECs, the cells were first incubated with iPS-EVs followed by a staurosporine treatment. Interestingly, we found that treatment of ECs with all types of iPS-EVs mediated strong cytoprotective effect in ECs (Figure 4C, right), suggesting the role of other molecular components of iPS-EVs—not only miR-126, in protecting ECs from apoptosis. These results from in vitro experiments indicate significant proangiogenic properties of iPS-miR-126-EVs when compared to unmodified iPS-EVs and their important functional impact on ECs including enhancement of metabolic activity and angiogenic and migratory capacity as well as survival in cytotoxic conditions, critical for ischemic tissue repair.

3.4 | iPS-miR-126-EVs improve blood perfusion and functional recovery of ischemic tissues in vivo

Following the findings from in vitro studies suggesting proangiogenic properties of iPS-miR-126-EVs, we investigated an impact of iPS-EVs on ischemic tissue recovery in vivo using murine model of acute hind limb ischemia. Human iPS-EVs were intramuscularly injected into immunodeficient SCID mice after ischemic limb injury induced by permanent femoral artery occlusion. Following ISEV recommendations for animal studies employing EVs,[30] we examined in vivo effects of our EV population of interest (iPS-miR-126-EVs), when compared to (i) EVs derived from native iPS cells (iPS-WT-EVs), (ii) "non-stem cell" EVs derived from adult maturated cells such as human skin fibroblasts (hSF-EVs), and (iii) PBS as a "vehicle" control.

During 28d of follow-up, we monitored animal condition and behavior as well as limb anatomical and functional condition by monitoring body mass, animal mobility, and macroscopic condition of injured limb. We showed that despite initial decrease in body weight and motility following the severe injury procedure, the animals in all groups regained their initial weight and activity at the end of experiment (at 28d), especially in the iPS-WT-EV- and iPS-miR-126-EV-treated groups (Figure S1). However, severe complications accompanying limb tissue ischemia such as limb necrosis and loss of toes or entire foot were observed

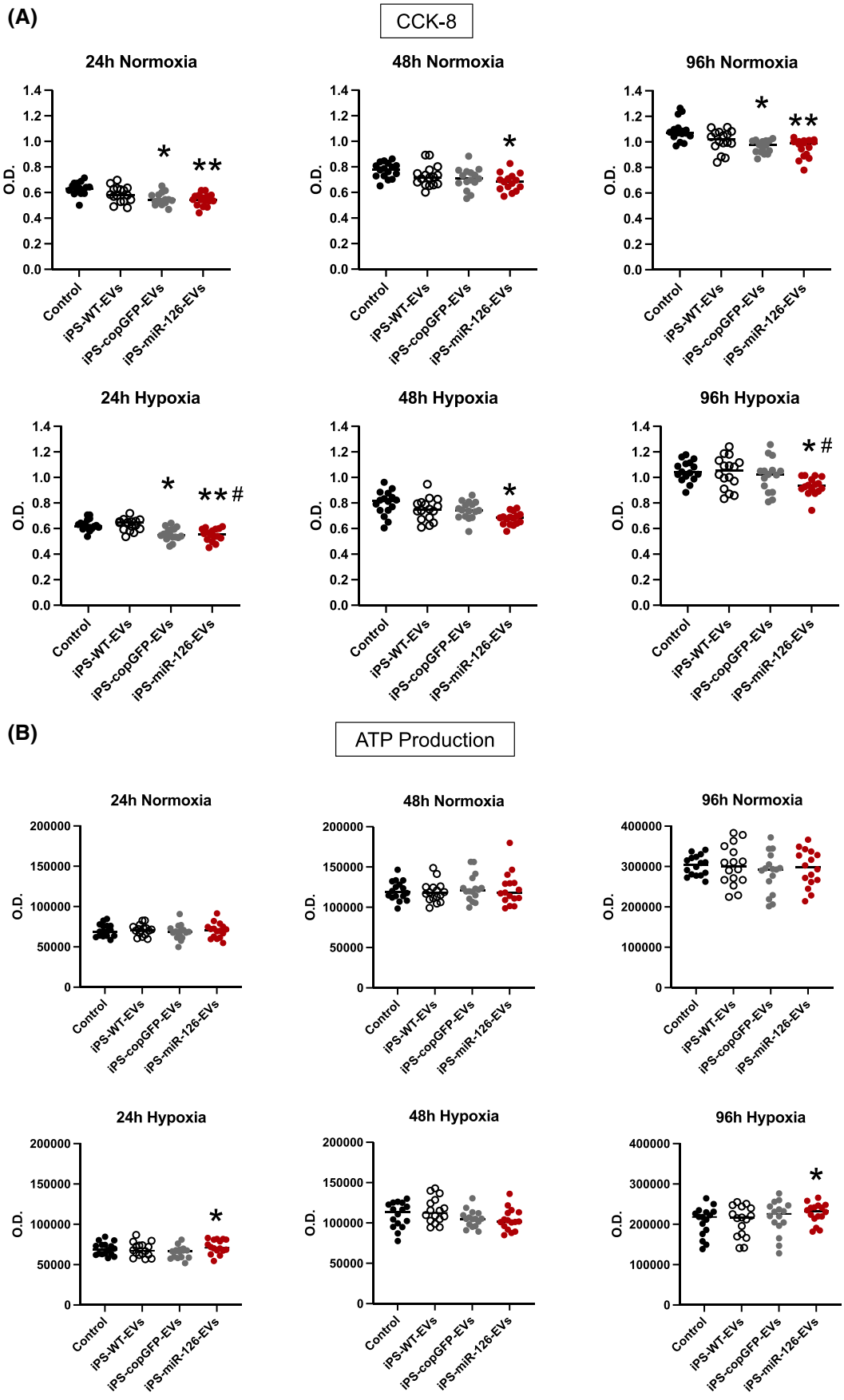

FIGURE 3 Proliferation and metabolic activity of ECs after treatment with iPS-EVs in vitro. Analysis of proliferation (CCK-8) (A) and metabolic activity (ATP Production) (B) of ECs following 24 h incubation with EVs. The analyses were performed at 24, 48, and 96 h after treatment of ECs with EVs and cultured in normoxic (upper panels) or hypoxic (1% O_2; lower panels) conditions. Mean values are indicated by black lines; $n = 16$; ANOVA with Tukey post-hoc test; comparison with iPS-WT-control cell lines; $^{*}p < .05$, $^{**}p < .01$; comparison with iPS-copGFP control cell line; $^{\#}p < .05$.

in animals from both vehicle- and hSF-EV-treated control groups (Figure S1, S2). Remarkably, neither limb necrosis nor tissue loss was observed in any animal treated with iPS-miR-126-EVs. Similarly, treatment with iPS-WT-EVs resulted in limb anatomical recovery, but a loss of toes was observed in some animals (Figure 5A).

Importantly, macroscopic observations correlated with quantitative results of blood perfusion measured in ischemic and non-ischemic limbs via laser Doppler system (Figure 5B,C). Our results showed severely impaired blood perfusion in injured limb at 24 h after femoral artery occlusion in all experimental groups (Figure 5B). However, at 14d and 21d post-EV treatment, we observed significantly improved blood perfusion in ischemic limbs of animals treated with iPS-miR-126-EVs, when compared to animals from other groups (Figure 5B).

Importantly, blood flow was slightly higher in EV-treated legs than in uninjured limbs, suggesting increased neovascularization and development of collateral circulation ongoing in ischemic tissue. We found increased blood perfusion also in animals treated with unmodified iPS-WT-EVs at 21d post-injury (Figure 5B), indicating also possible proangiogenic impact of other iPS-EV-derived molecular cargo. At 28d of follow-up, when only part of newly formed vessels was stabilized, we still observed a slightly higher perfusion in ischemic limbs of animals treated with iPS-miR-126-EVs, when compared to other groups.

Although condition of the limb was much better in iPS-WT-EVs transplanted group, when compared to the control (PBS), still 2 out of 6 animals has lost foot around day 14 post-injury. This is also the time point, when we saw highest difference between blood perfusion in iPS-WT-EVs and iPS-miR-126-EVs, and, remarkably, we did not observe any loss of foot or toes in iPS-miR-126-EVs; hence, we believe that miR-126 overexpression is beneficial (Figure 5D).

To identify possible molecular mechanisms involved in proangiogenic properties of iPS-miR-126-EVs after their transplantation in vivo, we measured expression of angiogenesis-related genes in injured tissues at 28d after EV injection using qPCR (Table S3). Our results revealed a distinct pattern of gene expression in tissues treated with iPS-WT-EVs and iPS-miR-126-EVs leading to upregulation of proangiogenic genes, when compared to PBS- and hSF-EV-treated controls where upregulation of profibrotic genes was predominantly observed (Figure 6A,B). We found several genes, which have been previously reported as important for EC proliferation, blood vessel formation, and growth,[34–37] being highly expressed in tissues following iPS-miR-126-EV administration, including angiopoietin, Tie-2, HIF-1α, MMP-9, TBX-1, TYPM, and PLG (Figure 6A,B). Additionally, several genes for growth factors involved in angiogenesis and new vessel formation and stabilization were highly expressed in tissues after treatment with iPS-miR-126-EVs, when compared to other groups, such as VEGFA, VEGFB, PDFGA, and CTGF.[38] Importantly, we found elevated expression of anti-angiogenic SERPINE1 and profibrotic TGFβ, TNF-SF, FGF-1, and FGF-6 in tissues harvested from animals treated with hSF-EVs, which factors may additionally inhibit endothelial cell proliferation and lead to their apoptosis.[39–41]

Taken together, in our in vivo experiment we found evidence that iPS-miR-126-EV transplantation into ischemic limb tissue provides effective tissue revascularization and leads to anatomical and functional recovery of injured ischemic organs, which is accompanied with upregulation of several genes guiding angiogenesis and EC functions.

To sum up our findings, we genetically modified human iPS cells to stably overexpress miR-126 and isolated EVs from these modified cells to study their effects on ECs both in vitro and in vivo. We determined the impact of iPS-EVs derived from miR-126-overexpressing cells (iPS-miR-126-EVs) on selected biological properties of human ECs in vitro, when compared with control iPS-EVs. We observed increased metabolic activity, survival under cytotoxic conditions, migration potential, and capillary formation capacity of ECs after iPS-miR-126-EV treatment. Injection of iPS-miR-126-EVs improved perfusion and limb anatomy and function in a murine model of acute limb ischemia in vivo. The improvement in ischemic limbs was accompanied by an increase in the expression of several angiogenesis-related genes in the treated tissues after iPS-miR-126-EV injection compared with controls. These results indicate that application of iPS-miR-126-EVs represents a novel and effective approach toward the treatment of ischemic tissues in vivo. These findings may lead to the development of new and safe iPS-EV-based therapies for ischemic tissue revascularization and repair to restore tissue function in patients with ischemic pathologies.

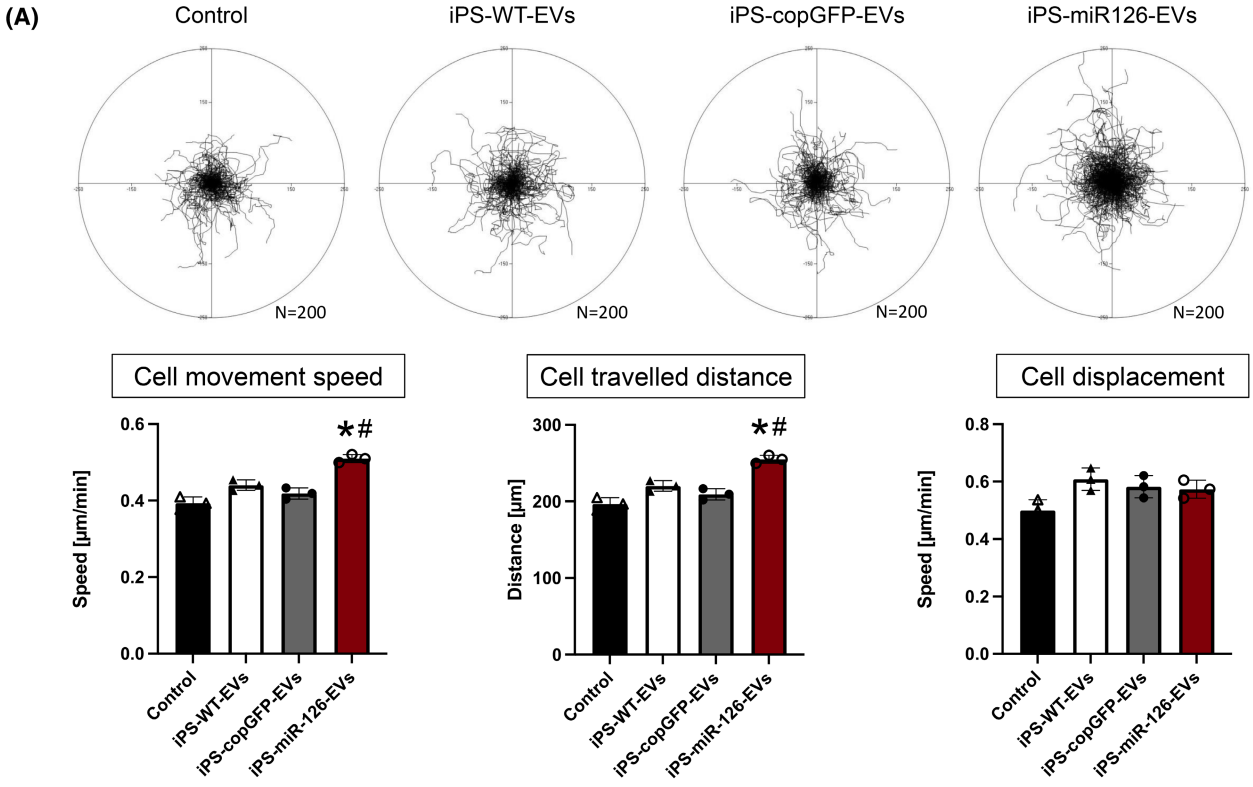

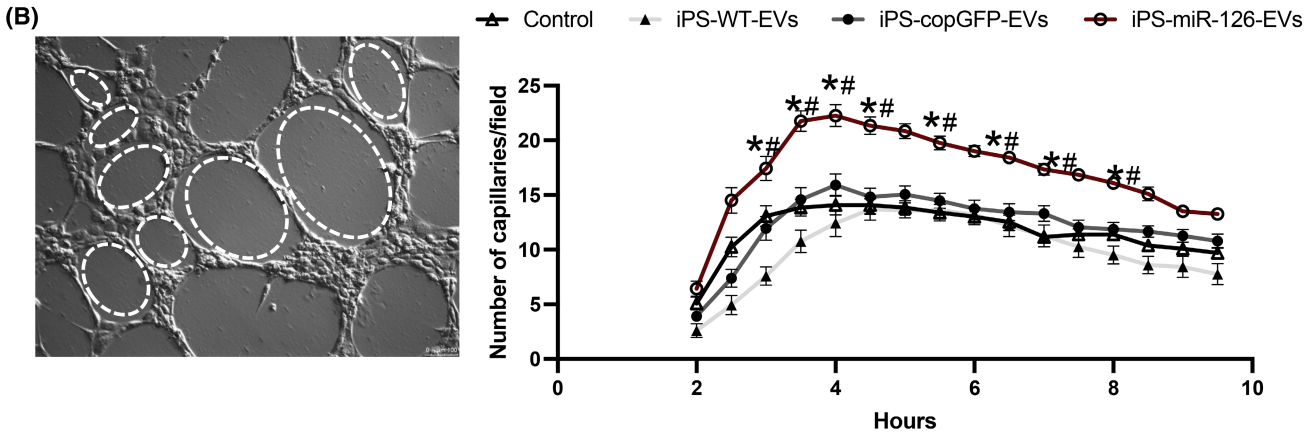

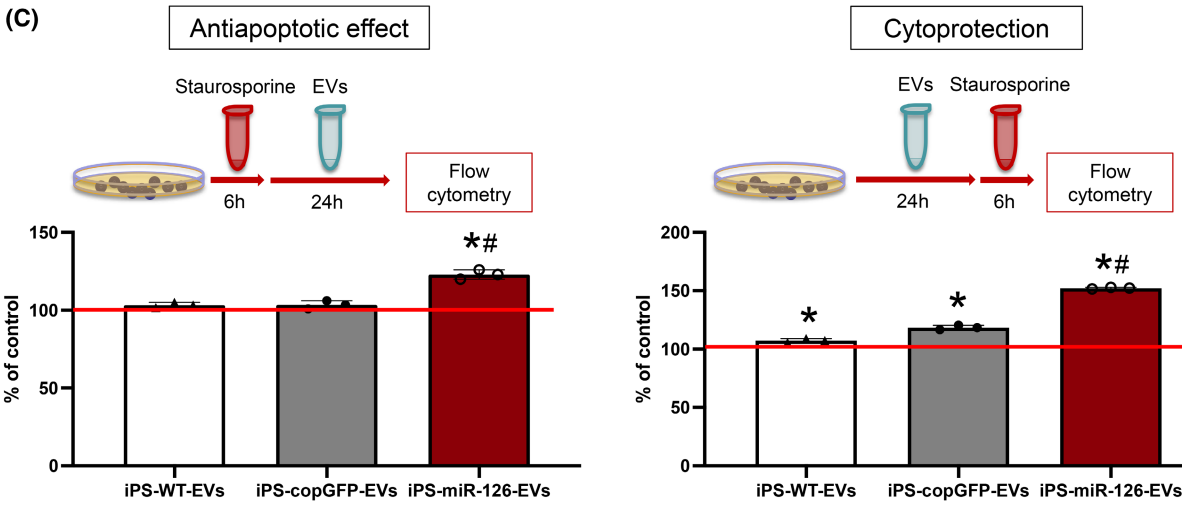

FIGURE 4 Impact of iPS-EVs on survival, migratory, and angiogenic capacity of ECs in vitro. (A) Analysis of EC migratory activity after iPS-EV treatment by microscopy. Cells were treated with iPS-EVs for 1 h, and their migration was recorded for 12 h at 10-min intervals. Two hundred different cells in each sample were analyzed. Representative cell trajectories of cardiac cells in tested conditions are presented in upper panel. Quantitative data of cell speed, distance, and displacement are presented in the lower panel. (B) Time-course analysis of angiogenic capacity of ECs on Matrigel. Exemplary photograph of capillaries formed by ECs with counting strategy. Graph presents quantitative analysis of capillary numbers per field of view, formed by ECs treated with different populations of iPS-EVs. (C) Analysis of anti-apoptotic (left panel) and cytoprotective (right panel) effects of iPS-EVs in ECs by flow cytometry with short schematics for each assay. Graphs show percentages of viable cells after treatment with various iPS-EVs when compared to control untreated cells. Red line indicates level of control (100%). Mean ± *SD*; $n = 3$; ANOVA with Tukey post-hoc test; comparison with iPS-WT-control cell lines; $^{*}p < .05$; comparison with iPS-copGFP control cell line; $^{\#}p < .05$.

4 | DISCUSSION

In our study, we demonstrated that EVs secreted by induced pluripotent stem cells and enriched in proangiogenic miR-126 modulate various endothelial cell functions and enhance their physiological angiogenic capacity in vitro and in vivo.

The abundance and severity of ischemic diseases including ischemic heart disease and critical limb ischemia still require development of new therapeutical strategies that would improve patient recovery and functional outcomes.[42] One of the adverse outcomes of tissue ischemia may be an irreversible loss of injured tissues occurring via cell necrosis or apoptosis due to restricted blood flow and oxygen supply.[43] Therefore, developing new, safe strategies for improved tissue revascularization remains an important challenge in therapy of ischemic tissue injuries.

Over the last years, growing evidence points at pro-regenerative and proangiogenic properties of extracellular vesicles released by various stem and progenitor cells,[9,10,44,45] including also iPS cells, which we have reported for the first time.[9,10,44] iPS cells possess capacity to give rise into any cell type and infinite ability to proliferate, resulting in their capability to produce a great number of extracellular vesicles, when compared to endothelial or mesenchymal stem cells.[46] iPS-EVs carry several molecules regulating other cell functional specification and behavior and such SC-derived EVs may also be potentially modified to enhance their activity by overexpression of selected factors, which is more challenging to achieve in matured cells in tissues or blood components.[47]

In our study, we attempted to enhance proangiogenic properties of iPS cell-derived EVs by overexpressing miR-126, which is an important regulator in various stages of blood vessel development and maturation.[14,15] We performed comprehensive functional studies to examine the impact of the iPS-miR-126-EVs on endothelial cell functions in vitro and their potential pro-regenerative effects in ischemic tissue in murine model of acute limb ischemia in vivo. Our results revealed, for the first time, significant proangiogenic properties of iPS-EVs enriched in miR-126 in vitro, as well as suggested pro-regenerative potential of iPS-EVs in in vivo in murine model of LI, which may further be advanced for the development of novel therapies of ischemic diseases.

We used iPS cells cultured in feeder-, xeno-, and serum-free conditions, which allowed us further isolation of "pure" iPS-EVs, avoiding contamination with compounds derived from other cell types or serum. We proved that miR-126 overexpression was effective in parental iPS cells and evaluated an impact of this modification on selected iPS cell properties. We have shown that miR-126 overexpression does not impact expression levels of early (FLK-1, TIE-2) and late (vWF, VE-CADH) angiogenesis-related genes, which was relatively high in both native and genetically modified iPS cells. However, the cells overexpressing miR-126 exhibited significantly higher expression of VEGF when compared to unmodified cells. We also found increased expression of proangiogenic genes in these cells when they were subjected to angiogenic differentiation in specific medium, which all together indicates their increased angiogenic capacity following miR-126 overexpression. It has been similarly reported by Jaafarpour et al. that overexpression of other selected miRNA, such as miR-375, was sufficient to initiate iPS differentiation toward hepatocytes.[48]

We next isolated EVs from native and genetically modified iPS cells with miR-126 expression using sequential centrifugation protocol and characterized them according to criteria recommended by ISEV.[30] TEM images confirmed the presence of small membrane vesicles in the samples, and submicron size was later confirmed via nanoparticle tracking analysis. We found that iPS-EVs form genetically modified cells were in average larger than the ones isolated from unmodified cells; however, currently there is no clear consensus whether biological cargo of EVs is related to the EV size.[49,50] There are some data though suggesting impact of genetic modification, transfection, staining, and electroporation on EV size as described by Joshi et al.[31]; however, no explanation has been given to said phenomenon.

EVs derived from both control and miR-126-overexpressing iPS cells represent heterogeneous populations consisting of both tetraspanins (CD81, CD63,

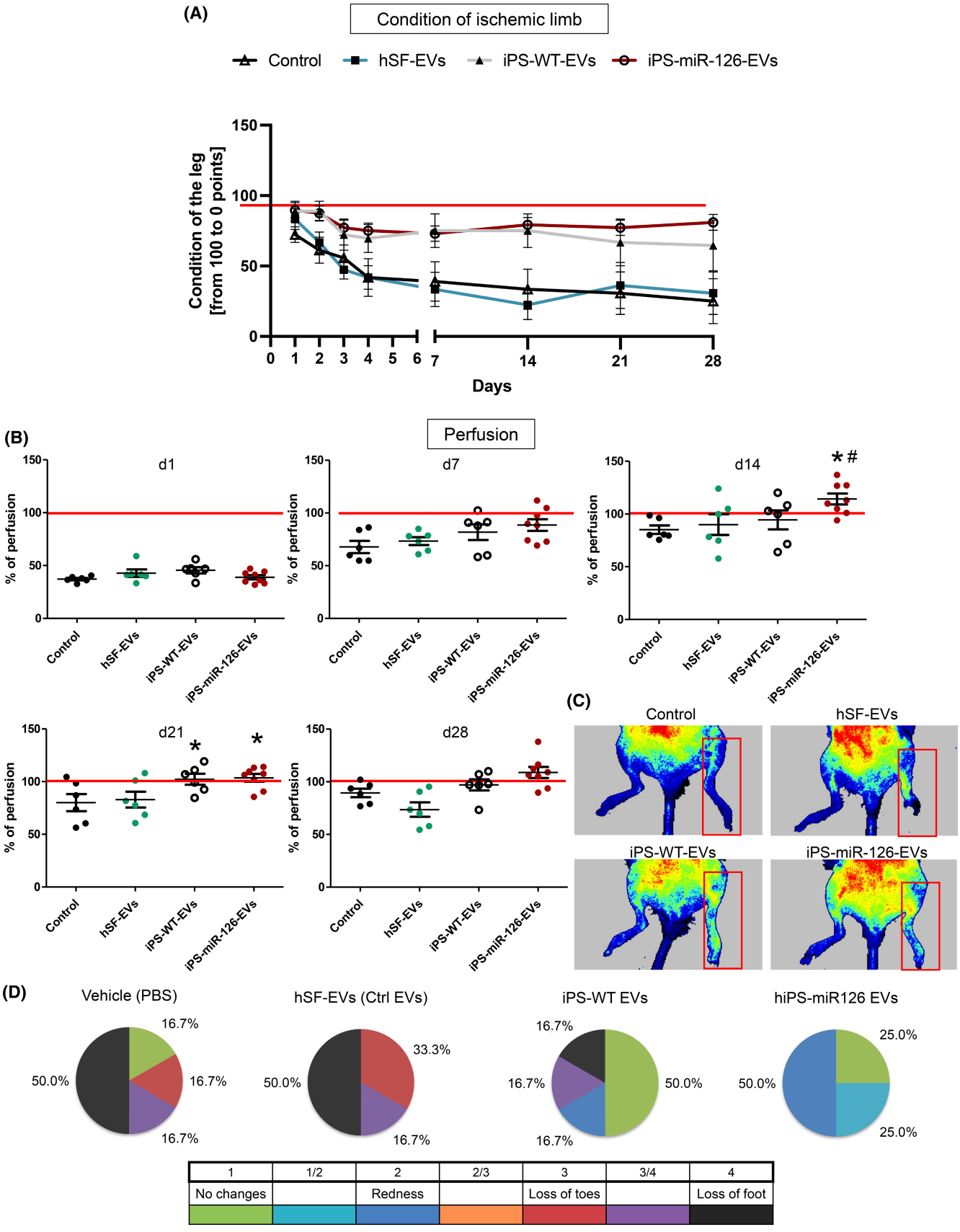

CD9) expressing exosomes and membrane proteins (SSEA-4) containing ectosomes. Consistently with other studies, we found that our iPS-EVs carry similar concentration of overexpressed miR-126 as well as other proangiogenic transcripts as parental cells.[8,10,51] Only vesicular VEGF levels were significantly elevated in

FIGURE 5 Impact of iPS-EV transplantation on ischemic limb condition and perfusion in vivo. (A) Semiquantitative analysis of ischemic limb condition evaluated by macroscopic observations at 1, 2, 3, 4, 7, 14, 21, and 28 days after iPS-EV treatment post-limb ischemia. Red line indicates values for control and non-ischemic limb. (B) Quantitative analysis of blood perfusion in ischemic leg measured by laser Doppler on 1, 7, 14, 21, and 28 days after iPS-EV treatment post-limb ischemia. Red line indicates perfusion in healthy, untreated legs (computed as 100%). Each dot represents data for a single animal in the group. Mean values with *SD* are indicated by black lines for each animal group. (C) Representative images of blood flow measured in ischemic and non-ischemic legs of animals in four experimental groups. Red box indicates the area of ischemic leg used for calculation the blood perfusion. Mean ± *SD*; $n = 6–8$ (in each group of animals); (D) Pie charts showing percentage differences in leg condition between control and experimental groups. Color legend presented as a table below. ANOVA with Tukey post-hoc test; comparison with vehicle (PBS)- treated control; $^{*}p < .05$; comparison with iPS-WT-EVs control cell line; $^{\#}p < .05$.

EVs, which potentially influenced their proangiogenic properties.

Since the overexpressed miR-126 was also found in genetically modified iPS-EVs, we evaluated the impact of iPS-miR-126-EVs on the functional properties of human coronary artery ECs in vitro, which represent optimal model of endothelial cells of a heart tissue in vitro, often affected by ischemia in vivo.[52,53] We observed that proliferation of ECs was inhibited in both normoxic and hypoxic conditions after treatment with iPS-miR-126-EVs, when compared to control EVs derived from unmodified iPS cells. Interestingly, the inhibitory effect of miR-126 on EC proliferation has been already suggested,[54] which may be accompanied with differentiation process initiated by miR-126. The increased maturation of the EV-treated ECs may be supported by the increased metabolic activity following treatment with iPS-miR-126-EVs in hypoxic conditions, which was measured by ATP production, and may also suggest beneficial use of iPS-EVs in treatment of ischemic tissues. Importantly, we found iPS-miR-126-EVs also enhancing EC migration, which is a critical EC activity in formation and sprouting of new blood vessels.[55] It is important to point out, that considering regular distance, that endothelial cell can cover in an hour, which is reported to be 10-15 μm/h[56]; 20% increase in cell speed and 15% increase in traveled distance that we observed in our study are considerably significant. It has been shown that migration of ECs may be stimulated in human tissues by growth factors such as VEGF, PDGF, or b-FGF, which factors may be regulated by miR-126 via its impact on, for example, HIF-1α expression.[55] Importantly, we found elevated expression of genes for the listed growth factors as well as HIF-1α in ischemic muscle tissues following iPS-miR-126-EV administration in vivo, supporting the important role of enhanced migratory capacity of ECs in new vessel formation in such ischemic tissues.

Among various methods evaluating cell angiogenic potential, the capillary formation assay on matrigel in vitro is one of the most commonly used in several studies.[57] We showed that ECs treated with iPS-miR-126-EVs formed more capillaries than cells treated with control EVs, which corresponds to previous reports from other groups showing that miR-126 increases proangiogenic EC capacity in vitro.[17,58] Interestingly, it has been shown that knock-out of miR-126 in ECs leads not only to decreased capacity in capillaries formation, but to their lower stability,[58] which suggest an impact of this miRNA on blood vessel maturation and stabilization that we also observed in our in vivo study. Finally, since the EC survival in hypoxic conditions would represent important factor enhancing the ischemic tissue and perfusion recovery, we evaluated an impact of iPS-EVs on ECs in cytotoxic conditions inducing cell apoptosis in vitro. We observed that treatment of ECs with iPS-EVs prior to the exposure to cytotoxic conditions inhibited apoptosis and this effect was present for both iPS-EVs derived from unmodified and genetically modified cells. We have previously also observed such cytoprotective effect of native iPS-EVs on human cardiac cells,[8] and this study indicated the phenomenon to be depended on other molecular cytoprotective factors rather than miR-126. However, importantly we found that iPS-miR-126-EVs reduced apoptosis of ECs after the exposure to cytotoxic agent, suggesting inhibitory activity of miR-126 on this process when the cells are already exposed to factors inducing apoptosis, which is much more relevant to clinical situation in patients. This finding may be crucial for treatment of patients after ischemic injury, when inhibition of apoptosis is critical for injured tissue survival and recovery.

Importantly, our clinically relevant data indicating proangiogenic potential of miR-126-overexpressing iPS-EVs in vitro, were also supported by our data obtained in vivo, in murine model of acute limb ischemia, which allowed us to evaluate functional and anatomical improvement of injured limb after the EV treatment. The model has been previously used in studies examining proangiogenic properties of cells and their derivatives isolated from various sources.[59,60] We followed ISEV guidelines for animal studies, using immunodeficient SCID mice transplanted with human-originated iPS-miR-126-EVs along with controls including unmodified iPS-EVs and "non-stem cell EVs" derived from mature cells such as skin fibroblasts. This allowed us to provide evidence that observed pro-regenerative and proangiogenic effects were specific to

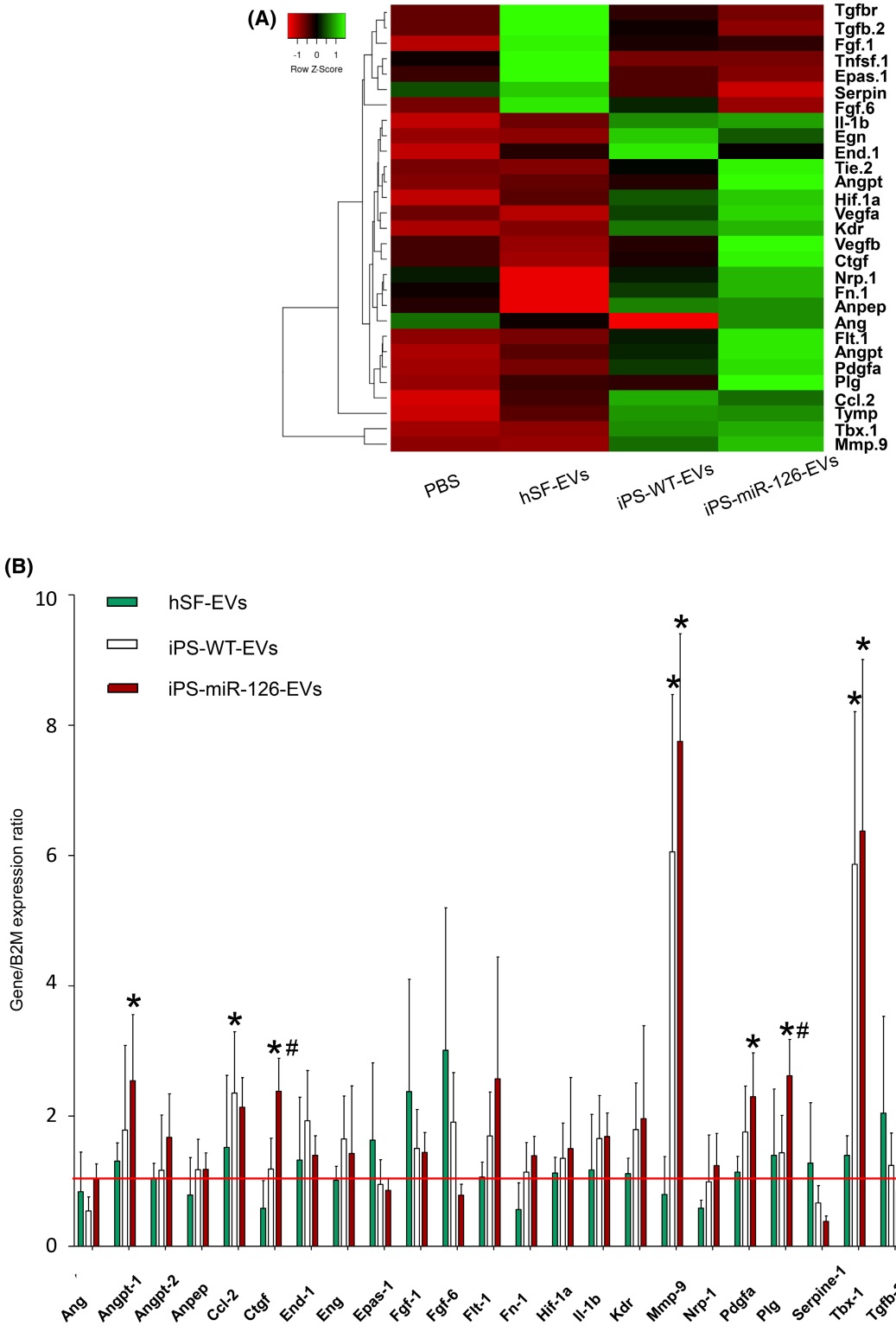

FIGURE 6 Analysis of selected gene expression in murine ischemic muscles tissue after iPS-EV transplantation. (A) Heatmap representation of the relative mean expression of selected indicated genes analyzed in ischemic muscle tissues at 28d after iPS-EV treatment, by RT-qPCR. The expression level of selected genes is presented from the lowest (red) to the highest (green), based on the Row Z-Score parameter generated by Heatmapper Software. (B) Quantitative selected gene expression analysis in ischemic murine muscles at 28 days post-iPS-EV treatment. Data were calculated as a fold change in the gene expression when compared to control (PBS) and are presented as the mean ± *SD*. The red line indicates the level of the indicated gene expression in control (computed as 1). Mean ± *SD*; $n = 6–8$; ANOVA with Tukey post-hoc test; comparison with vehicle (PBS)-treated control; $^{*}p < .05$; comparison with iPS-WT-EV control cell line; $^{\#}p < .05$.

our stem cell-derived EVs with miR-126 overexpression. Remarkably, we showed that animals, which received iPS cell-derived EVs, including the ones overexpressing miR-126, recovered faster functionally and did not suffer severe ischemia-related complications such as lose of toes and feet due to tissue necrosis, when compared to control animals treated with vehicle- or fibroblast-derived EVs.[61] Blood perfusion in injured animal legs was monitored using clinically relevant laser Doppler system. Improved blood flow was observed in ischemic muscle tissue after treatment with iPS-miR-126-EVs early (7 days) after transplantation. Interestingly, when measured two weeks after the EV injection, the blood perfusion in ischemic limb was even higher than in uninjured healthy leg, suggesting intensive neovascularization stimulated by EVs. We still observed higher blood perfusion in both iPS-miR-126-EV- and iPS-WT-EV-treated animals when compared to controls at later time points (at days 21 and 28), but only part of the newly formed vessels were stabilized, which corresponds to normal and physiological process of blood vessel development and maturation.[62] Since the adult, but still relatively young animals used in this study exhibited endogenous capacity for blood flow recovery, potential use of older animals in the future studies could even greater highlight the pro-regenerative capacity of the EVs.

Molecular analysis of ischemic tissues after iPS-EV transplantation revealed increase in expression of several proangiogenic genes in treated muscle tissues when compared to control animals, especially when miR-126-overexpressing iPS-EVs were administrated. The up-regulated genes include MMP-9 and TBX-1, which are involved in blood vessel formation during embryogenesis and tissue neovascularization after ischemic injury.[34,36] Interestingly, it has been reported that miR-126 is a regulator of MMP-9 expression,[63,64] while its impact on TBX-1 levels was not described before. We also found several genes regulating endothelial cell proliferation and blood vessel formation to be highly expressed in ischemic muscle tissues after treatment with miR-126-overexpressing iPS-EVs, including angiopoietin, Tie-2, HIF-1α, TYPM, and PLG.[35,37] Additionally, genes for critical growth factors guiding angiogenesis, new vessel formation, and maturation such as VEGFA, VEGFB, PDFGA, and CTGF[38] were also activated in muscle tissues after treatment with iPS-miR-126-EVs, suggesting their potential proangiogenic effects in vivo. Importantly, changes in expression of selected proangiogenic genes, that we also observed in our study, can be directly linked to high miR-126 levels. This was reported before for expression of MMP-9,[64] ANGPT-1 and ANGPT-2,[17] PDGFA,[38] and TIE2.[65]

On the other hand, we found increased expression of genes for anti-angiogenic SERPINE1 along with several profibrotic factors such as TGFβ, TNF-SF, FGF-1, and FGF-6 in ischemic tissues after treatment with skin fibroblast-derived EVs. Based on our search through miRDB, we were able to establish that TGFBR, FGF1, and SERPIN are miR-126-5p targets that are down-regulated in our study, in animals from iPS-miR-126-EV- treated group. These factors may adversely impact endothelial cell proliferation and survival,[39–41] but support the observations that the type of parental cells for EV specimens determines their functional activity on target cells and tissues.

Our results confirmed that iPS cell-derived EVs, both iPS-WT-EVs and especially iPS-miR-126-EVs, exhibit pro-regenerative potential, when administered to animals in murine model of limb ischemia. They stimulate pro-regenerative processes in ischemic tissue, including the ones depending on EC activity, which may be related to the molecular cargo of such vesicles released by pluripotent SCs with a high capacity for regulating developmental processes and tissue repair. Such effects were not observed when mature fibroblast-derived EVs were used for treatment, and only upregulation of genes typical for the functional activity of such maturated cells was observed in the ischemic tissue, without any therapeutic effects observed after such treatment.

5 | CONCLUSIONS

Our data indicate that EVs released by induced pluripotent stem cells and enriched in miR-126 may modulate endothelial cell functions, including in ischemic tissue by enhancing their physiological capacity in angiogenesis and new vessel formation. The iPS-miR-126-EV treatment of ECs leads to their better survival in cytotoxic conditions as well as to enhanced metabolic activity, migratory capacity, and angiogenic potential in vitro, which favors EC-related angiogenesis and tissue neovascularization in vivo. Treatment of ischemic tissues with iPS-miR-126-EVs in vivo results with greater blood perfusion the tissues accompanied with increase in expression of several proangiogenic genes, which may be linked with accelerated recovery of blood perfusion in injured tissue and functional improvement of ischemic organ. Thus, use of iPS-EVs enriched in proangiogenic molecular factors such as miR-126 may be a future approach to enhance ischemic tissue repair.

AUTHOR CONTRIBUTIONS

Katarzyna Kmiotek-Wasylewska designed and performed most of the in vitro experiments, collected, analyzed and interpreted the data; prepared figures and draft of the manuscript, and participated in preparing the final version of the manuscript. Anna Łabędź-Masłowska designed

and performed in vivo experiment, collected and analyzed data. Sylwia Bobis-Wozowicz prepared iPS cell lines and performed their genetic analyses. Elżbieta Karnas performed analyses of EV specimens with flow cytometric platforms and NTA. Sylwia Noga assisted in in vivo study and performed data analysis. Małgorzata Sekuła-Stryjewska supported the in vitro stem cell cultures. Olga Woźnicka performed EV imaging with TEM. Zbigniew Madeja provided access to infrastructure and methodology for cell migration analysis. Buddhadeb Dawn provided supervision and methodology for in vivo study. Ewa Zuba-Surma designed and supervised the entire study; analyzed and interpreted data and prepared the final version of the manuscript.

ACKNOWLEDGMENTS

This work was supported by the National Science Centre of Poland under grants PRELUDIUM no. 2016/21/N/NZ3/00363 to K.K-W and MAESTRO no. 2019/34/A/NZ3/00134 to E.Z-S.

The open-access publication has been supported by the Faculty of Biochemistry, Biophysics and Biotechnology under the Strategic Programme Excellence Initiative at Jagiellonian University in Krakow, Poland.

DISCLOSURES

The authors declare no financial or non-financial interests that are directly or indirectly related to the work submitted for publication.

DATA AVAILABILITY STATEMENT

The data and materials generated during this study are available from the corresponding author upon request to any qualified researcher.

DECLARATION OF GENERATIVE AI AND AI-ASSISTED TECHNOLOGIES IN THE WRITING PROCESS

The authors declare no use of AI and AI-assisted technologies in the writing process of the article.

ORCID

Katarzyna Kmiotek-Wasylewska https://orcid.org/0000-0001-6298-2853
Anna Łabędź-Masłowska https://orcid.org/0000-0002-8088-6221
Sylwia Bobis-Wozowicz https://orcid.org/0000-0002-2200-6767
Elżbieta Karnas https://orcid.org/0000-0001-9956-1593
Sylwia Noga https://orcid.org/0000-0003-4475-187X
Małgorzata Sekuła-Stryjewska https://orcid.org/0000-0002-9511-9498
Olga Woźnicka https://orcid.org/0000-0002-7500-5047
Zbigniew Madeja https://orcid.org/0000-0002-5523-1215
Buddhadeb Dawn https://orcid.org/0000-0001-5890-115X
Ewa K. Zuba-Surma https://orcid.org/0000-0001-6814-6127

REFERENCES

1. Nowbar AN, Gitto M, Howard JP, Francis DP, Al-Lamee R. Mortality from ischemic heart disease. *Circ Cardiovasc Qual Outcomes*. 2019;12:e005375.
2. Kasai-Brunswick TH, Carvalho AB, Campos de Carvalho AC. Stem cell therapies in cardiac diseases: current status and future possibilities. *World J Stem Cells*. 2021;13:1231-1247.
3. Yu H, Lu K, Zhu J, Wang J. Stem cell therapy for ischemic heart diseases. *Br Med Bull*. 2017;121:135-154.
4. Li X, Tamama K, Xie X, Guan J. Improving cell engraftment in cardiac stem cell therapy. *Stem Cells Int*. 2016;2016:7168797.
5. Tenreiro MF, Louro AF, Alves PM, Serra M. Next generation of heart regenerative therapies: progress and promise of cardiac tissue engineering. *NPJ Regen Med*. 2021;6:1-17.
6. Bjorge IM, Kim SY, Mano JF, Kalionis B, Chrzanowski W. Extracellular vesicles, exosomes and shedding vesicles in regenerative medicine—a new paradigm for tissue repair. *Biomater Sci*. 2017;6:60-78.
7. Hullin-Matsuda F, Colosetti P, Rabia M, Luquain-Costaz C, Delton I. Exosomal lipids from membrane organization to biomarkers: focus on an endolysosomal-specific lipid. *Biochimie*. 2022;203:77-92.
8. Adamiak M, Cheng G, Bobis-Wozowicz S, et al. Induced pluripotent stem cell (iPSC)-derived extracellular vesicles are safer and more effective for cardiac repair than iPSCs. *Circ Res*. 2018;122:296-309.
9. Bobis-Wozowicz S, Kmiotek K, Kania K, et al. Diverse impact of xeno-free conditions on biological and regenerative properties of hUC-MSCs and their extracellular vesicles. *J Mol Med (Berl)*. 2017;95:205-220.
10. Bobis-Wozowicz S, Kmiotek K, Sekula M, et al. Human induced pluripotent stem cell-derived microvesicles transmit RNAs and proteins to recipient mature heart cells modulating cell fate and behavior. *Stem Cells*. 2015;33:2748-2761.
11. Correia de Sousa M, Gjorgjieva M, Dolicka D, Sobolewski C, Foti M. Deciphering miRNAs' action through miRNA editing. *Int J Mol Sci*. 2019;20:1-22.
12. Dhahbi JM, Atamna H, Boffelli D, Magis W, Spindler SR, Martin DI. Deep sequencing reveals novel microRNAs and regulation of microRNA expression during cell senescence. *PLoS One*. 2011;6:e20509.
13. Ouyang Z, Wei K. miRNA in cardiac development and regeneration. *Cell Regen*. 2021;10:1-21.
14. Kuhnert F, Mancuso MR, Hampton J, et al. Attribution of vascular phenotypes of the murine Egfl7 locus to the microRNA miR-126. *Development*. 2008;135:3989-3993.
15. Wang S, Aurora AB, Johnson BA, et al. The endothelial-specific microRNA miR-126 governs vascular integrity and angiogenesis. *Dev Cell*. 2008;15:261-271.
16. Jansen F, Yang X, Hoelscher M, et al. Endothelial microparticle-mediated transfer of MicroRNA-126 promotes

vascular endothelial cell repair via SPRED1 and is abrogated in glucose-damaged endothelial microparticles. *Circulation*. 2013;128:2026-2038.
17. Sessa R, Seano G, di Blasio L, et al. The miR-126 regulates angiopoietin-1 signaling and vessel maturation by targeting p85beta. *Biochim Biophys Acta*. 2012;1823:1925-1935.
18. Li SQ, Yi ZH, Li MQ, Zhu ZL. Baicalein improves the chemoresistance of ovarian cancer through regulation of CirSLC7A6. *J Ovarian Res*. 2023;16:1-16.
19. Li M, Zhang Z, Guan L, Ji S, Lu P. ERH gene knockdown inhibits the proliferation and migration of ARPE-19 cells through MCM complex and EMT process. *Gene*. 2024;892:1-10.
20. Donovan D, Brown NJ, Bishop ET, Lewis CE. Comparison of three in vitro human 'angiogenesis' assays with capillaries formed in vivo. *Angiogenesis*. 2001;4:113-121.
21. Fan Y, Lu H, Liang W, et al. Endothelial TFEB (transcription factor EB) positively regulates postischemic angiogenesis. *Circ Res*. 2018;122:945-957.
22. Tabit CE, Chen P, Kim GH, et al. Elevated angiopoietin-2 level in patients with continuous-flow left ventricular assist devices leads to altered angiogenesis and is associated with higher nonsurgical bleeding. *Circulation*. 2016;134:141-152.
23. Gouin K, Peck K, Antes T, et al. A comprehensive method for identification of suitable reference genes in extracellular vesicles. *J Extracell Vesicles*. 2017;6:1-11.
24. Lovasova V, Bem R, Chlupac J, et al. Animal experimental models of ischemic limbs—a systematic review. *Vascul Pharmacol*. 2023;153:1-12.
25. Guo L, Yang Q, Wei R, et al. Enhanced pericyte-endothelial interactions through NO-boosted extracellular vesicles drive revascularization in a mouse model of ischemic injury. *Nat Commun*. 2023;14:1-18.
26. Lu H, Yuan P, Ma X, et al. Angiotensin-converting enzyme inhibitor promotes angiogenesis through Sp1/Sp3-mediated inhibition of notch signaling in male mice. *Nat Commun*. 2023;14:731.
27. Niiyama H, Huang NF, Rollins MD, Cooke JP. Murine model of hindlimb ischemia. *J Vis Exp*. 2009;23:1-14.
28. Apte RS, Chen DS, Ferrara N. VEGF in signaling and disease: beyond discovery and development. *Cell*. 2019;176:1248-1264.
29. Shibuya M. Vascular endothelial growth factor (VEGF) and its receptor (VEGFR) signaling in angiogenesis: a crucial target for anti- and pro-angiogenic therapies. *Genes Cancer*. 2011;2:1097-1105.
30. Thery C, Witwer KW, Aikawa E, et al. Minimal information for studies of extracellular vesicles 2018 (MISEV2018): a position statement of the International Society for Extracellular Vesicles and update of the MISEV2014 guidelines. *J Extracell Vesicles*. 2018;7:1535750.
31. Joshi BS, Ortiz D, Zuhorn IS. Converting extracellular vesicles into nanomedicine: loading and unloading of cargo. *Materials Today Nano*. 2021;16:1-23.
32. Mathieu M, Nevo N, Jouve M, et al. Specificities of exosome versus small ectosome secretion revealed by live intracellular tracking of CD63 and CD9. *Nat Commun*. 2021;12:4389.
33. Wang WY, Lin D, Jarman EH, Polacheck WJ, Baker BM. Functional angiogenesis requires microenvironmental cues balancing endothelial cell migration and proliferation. *Lab Chip*. 2020;20:1153-1166.
34. Cioffi S, Martucciello S, Fulcoli FG, et al. Tbx1 regulates brain vascularization. *Hum Mol Genet*. 2014;23:78-89.
35. Li W, Yue H. Thymidine phosphorylase: a potential new target for treating cardiovascular disease. *Trends Cardiovasc Med*. 2018;28:157-171.
36. Mira E, Lacalle RA, Buesa JM, et al. Secreted MMP9 promotes angiogenesis more efficiently than constitutive active MMP9 bound to the tumor cell surface. *J Cell Sci*. 2004;117:1847-1857.
37. Oh CW, Hoover-Plow J, Plow EF. The role of plasminogen in angiogenesis in vivo. *J Thromb Haemost*. 2003;1:1683-1687.
38. Roy H, Bhardwaj S, Yla-Herttuala S. Biology of vascular endothelial growth factors. *FEBS Lett*. 2006;580:2879-2887.
39. Fajardo LF, Kwan HH, Kowalski J, Prionas SD, Allison AC. Dual role of tumor necrosis factor-alpha in angiogenesis. *Am J Pathol*. 1992;140:539-544.
40. Ferrari G, Cook BD, Terushkin V, Pintucci G, Mignatti P. Transforming growth factor-beta 1 (TGF-beta1) induces angiogenesis through vascular endothelial growth factor (VEGF)-mediated apoptosis. *J Cell Physiol*. 2009;219:449-458.
41. Wu J, Strawn TL, Luo M, et al. Plasminogen activator inhibitor-1 inhibits angiogenic signaling by uncoupling vascular endothelial growth factor receptor-2-alphaVbeta3 integrin cross talk. *Arterioscler Thromb Vasc Biol*. 2015;35:111-120.
42. Khan MA, Hashim MJ, Mustafa H, et al. Global epidemiology of ischemic heart disease: results from the global burden of disease study. *Cureus*. 2020;12:e9349.
43. Cowled P, Fitridge R. Pathophysiology of reperfusion injury. In: Fitridge R, Thompson M, eds. *Mechanisms of Vascular Disease: A Reference Book for Vascular Specialists*. Adelaide (AU); 2011.
44. Bian S, Zhang L, Duan L, Wang X, Min Y, Yu H. Extracellular vesicles derived from human bone marrow mesenchymal stem cells promote angiogenesis in a rat myocardial infarction model. *J Mol Med (Berl)*. 2014;92:387-397.
45. Dumbrava DA, Surugiu R, Borger V, et al. Mesenchymal stromal cell-derived small extracellular vesicles promote neurological recovery and brain remodeling after distal middle cerebral artery occlusion in aged rats. *Geroscience*. 2022;44:293-310.
46. Williams R. Induced pluripotent stem cells and the promise of proliferation. *Circ Res*. 2009;105:1159-1161.
47. Tan PH, Xue SA, Manunta M, et al. Effect of vectors on human endothelial cell signal transduction: implications for cardiovascular gene therapy. *Arterioscler Thromb Vasc Biol*. 2006;26:462-467.
48. Jaafarpour Z, Soleimani M, Hosseinkhani S, et al. Overexpression of microRNA-375 and microRNA-122 promotes the differentiation of human induced pluripotent stem cells into hepatocyte-like cells. *Biologicals*. 2020;63:24-32.
49. Bobrie A, Colombo M, Krumeich S, Raposo G, Thery C. Diverse subpopulations of vesicles secreted by different intracellular mechanisms are present in exosome preparations obtained by differential ultracentrifugation. *J Extracell Vesicles*. 2012;1:1-11.
50. Brennan K, Martin K, FitzGerald SP, et al. A comparison of methods for the isolation and separation of extracellular vesicles from protein and lipid particles in human serum. *Sci Rep*. 2020;10:1-13.
51. Qiu G, Zheng G, Ge M, et al. Mesenchymal stem cell-derived extracellular vesicles affect disease outcomes via transfer of microRNAs. *Stem Cell Res Ther*. 2018;9:320.

52. Chiu CZ, Wang BW, Yu YJ, Shyu KG. Hyperbaric oxygen activates visfatin expression and angiogenesis via angiotensin II and JNK pathway in hypoxic human coronary artery endothelial cells. *J Cell Mol Med*. 2020;24:2434-2443.
53. Pandey AK, Singhi EK, Arroyo JP, et al. Mechanisms of VEGF (vascular endothelial growth factor) inhibitor-associated hypertension and vascular disease. *Hypertension*. 2018;71:e1-e8.
54. Ebrahimi F, Gopalan V, Smith RA, Lam AK. miR-126 in human cancers: clinical roles and current perspectives. *Exp Mol Pathol*. 2014;96:98-107.
55. Lamalice L, Le Boeuf F, Huot J. Endothelial cell migration during angiogenesis. *Circ Res*. 2007;100:782-794.
56. Szabo A, Unnep R, Mehes E, et al. Collective cell motion in endothelial monolayers. *Phys Biol*. 2010;7:046007.
57. Garrido T, Riese HH, Aracil M, Perez-Aranda A. Endothelial cell differentiation into capillary-like structures in response to tumour cell conditioned medium: a modified chemotaxis chamber assay. *Br J Cancer*. 1995;71:770-775.
58. Fish JE, Santoro MM, Morton SU, et al. miR-126 regulates angiogenic signaling and vascular integrity. *Dev Cell*. 2008;15:272-284.
59. Brenes RA, Jadlowiec CC, Bear M, et al. Toward a mouse model of hind limb ischemia to test therapeutic angiogenesis. *J Vasc Surg*. 2012;56:1669-1679; discussion 1679.
60. Ranghino A, Cantaluppi V, Grange C, et al. Endothelial progenitor cell-derived microvesicles improve neovascularization in a murine model of hindlimb ischemia. *Int J Immunopathol Pharmacol*. 2012;25:75-85.
61. Westvik TS, Fitzgerald TN, Muto A, et al. Limb ischemia after iliac ligation in aged mice stimulates angiogenesis without arteriogenesis. *J Vasc Surg*. 2009;49:464-473.
62. Logsdon EA, Finley SD, Popel AS, Mac Gabhann F. A systems biology view of blood vessel growth and remodelling. *J Cell Mol Med*. 2014;18:1491-1508.
63. Yang W, Shang X, Jiang B. Application values of MMP-9 and miR-126 detection for diagnosis of coronary heart disease in hypertensive patients. *Int J Clin Exp Med*. 2019;12:12896-12903.
64. Ye P, Liu J, He F, Xu W, Yao K. Hypoxia-induced deregulation of miR-126 and its regulative effect on VEGF and MMP-9 expression. *Int J Med Sci*. 2014;11:17-23.
65. Matkar PN, Cao WJ, Rudenko D, Chen HH, Kuliszewski MA, Leong-Poi H. The MIR-126/VEGFR-2 and MIR-126/TIE2 axes promote early and late angiogenesis in chronic hindlimb ischemia. *Can J Cardiol*. 2015;31:S229-S230.

SUPPORTING INFORMATION

Additional supporting information can be found online in the Supporting Information section at the end of this article.

How to cite this article: Kmiotek-Wasylewska K, Łabędź-Masłowska A, Bobis-Wozowicz S, et al. Induced pluripotent stem cell-derived extracellular vesicles enriched with miR-126 induce proangiogenic properties and promote repair of ischemic tissue. *The FASEB Journal*. 2024;38:e23415. doi:10.1096/fj.202301836R